The Journal of Experimental Biology 215, 2703-2710

doi:10.1242/jeb.063958

RESEARCH ARTICLE

Functional implications of morphological specializations among the pectoral fin rays of the benthic longhorn sculpin

Natalia K. Taft* and Benjamin N. Taft

Department of Organismic and Evolutionary Biology, 319 Morrill Science Center South, University of Massachusetts Amherst, 611 N. Pleasant Street, Amherst, MA 01003, USA

*Author for correspondence at present address: Department of Biological Sciences, University of Wisconsin-Parkside, 900 Wood Road, PO Box 2000 Kenosha, WI 53141-2000, USA (taft.nk@gmail.com)

SUMMARY

Fin ray structure in ray-finned fishes (Actinopterygii) largely defines fin function. Fin rays convert the muscle activity at the base of the fin to shape changes throughout the external fin web. Despite their critical functional significance, very little is known about the relationship between form and function in this key vertebrate structure. In this study we demonstrate that morphological specializations of the pectoral fin rays of the benthic longhorn sculpin (*Myoxocephalus octodecimspinosus*) have specific functional consequences both within and among individual rays. The fin rays of longhorn sculpin have an elongate unjointed region with a cylindrical shape in cross-section proximally, and are jointed with a crescent-shaped cross-section distally. Variation in the relative length of the proximal *versus* distal regions affects the location of maximum curvature as well as the mean curvature along the length of individual rays. We experimentally manipulated fin rays to mimic the differential muscle activity that generates curvature of fin rays in living animals. We found that the shape of the fin rays in cross-section affects their curvature. Among fin rays, the most ventral fin rays with relatively longer proximal unjointed regions have a more distal location of maximum curvature. These ventral rays also have higher mean curvature, likely because of a combination of features including the cross-sectional shape, area and diameter of the distal segments as well as their relative size and number, which were not examined in detail here. Because these rays are used routinely for substrate contact, this higher curvature could contribute to increased flexibility for substrate contact behaviors such as clinging or gripping the substrate. These morphological and functional differences among fin rays are correlated with the functional regionalization of the fin. Specifically, the ventral fin rays that are used during substrate contact are more stiff proximally and more highly curved distally than the pectoral rays in the dorsal region, which are longer and used during slow swimming. This study highlights the importance of examining morphological and functional variation both within and among complex structures such as fin rays.

Key words: pectoral fin, fin ray, lepidotrichia, second moment of area, bending, sculpin.

Received 9 August 2011; Accepted 16 April 2012

INTRODUCTION

The ray-finned fishes (Actinopterygii) are named for the bony dermal fin rays, or lepidotrichia, that support the external fin web. Ray-finned fishes have a high degree of control over the curvature and relative position of individual fin rays, which define the shape of the fin surface as a whole (Alben et al., 2007; Lauder et al., 2006). This flexibility supports a wide range of fin-based behaviors including, but not limited to, propulsion, maneuvering and hovering in the water column as well as hopping, perching and digging into the substrate. Despite their crucial functional role, very little is known about the diversity of form and function of fin rays.

The morphology and bending properties of the fin rays of pelagic fishes have been described in detail in a small number of studies (Goodrich, 1904; Geerlink and Videler, 1987; Alben et al., 2007; Taft, 2011). Lepidotrichia are made up of two segmented bony halves called hemitrichia (singular 'hemitrich') (Goodrich, 1904; Geerlink and Videler, 1987; Alben et al., 2007; Lauder et al., 2011). The sister hemitrichia are joined by collagenous fibers that run perpendicular to the long axis of the rays (Geerlink and Videler, 1987). Each hemitrich has a short proximal, unsegmented region that serves as the attachment site for the muscles that control the relative position and curvature of the individual rays. The remainder of the length of each ray consists of crescent-shaped segments connected by collagenous joints (Geerlink and Videler, 1987; Alben et al., 2007). The segments of the sister hemitrichia are oriented with their concave surfaces facing each other, giving the fin ray the form of a hollow cylinder in cross-section for most of its length (Gosline, 1973; Gosline, 1994; Geerlink and Videler, 1987; Alben et al., 2007; Taft, 2011).

Curvature of the individual lepidotrichia is generated by the activity of muscles that originate on the pectoral girdle and insert onto the proximal base of each hemitrich. Muscle contraction on the medial or lateral hemitrich causes the sister hemitrichia to slide past one another. Simultaneous rotation of the joints between adjacent segments generates bending along the length of the fin ray. This differential muscle activity controls the curvature and relative position of the fin rays, causing the fin to be spread, closed, abducted or adducted (Geerlink and Videler, 1987; Alben et al., 2007; Lauder et al., 2011). The curvature of individual fin rays is largely independent of the curvature of the adjacent rays, despite the fact that they are connected by fin webbing (Standen and Lauder, 2005). Because the muscles that control ray curvature are at the base of

the fin, the morphology of the lepidotrichia defines their flexibility and, by extension, that of the fin as a whole (Lauder and Madden, 2007).

Fin ray morphology varies among pelagic and benthic fishes. The pelagic fishes in which fin ray morphology has been studied in the most detail are the Nile tilapia, *Oreochromis niloticus* (Geerlink and Videler, 1987), and the bluegill sunfish, *Lepomis macrochirus* (Lauder et al., 2011), which use their paired fins to interact exclusively with water. In contrast, the fins of benthic fishes are used to interact with a variety of solid substrates as well as with water. Fin rays that perform routine substrate-contact behaviors require increased flexibility (distally) and/or increased stiffness (proximally) relative to those of pelagic species. For example, two benthic species, the father lasher (*Myoxocephalus scorpious*) and the plaice (*Pleuronectes platessa*), have been shown to use their fin rays like 'fingers' to curve around and grip the substrate to help resist displacement from the substrate (Webb, 1989). Both species use their fin rays for this purpose despite very different body shapes. This gripping behavior requires a high degree of flexibility in the fin rays that are used in this manner, the anterior ventral rays in the father lasher, and the median fins of the plaice (Webb, 1989). This behavior has also been described in blennies (Brandstätter et al., 1990), in which it has also been hypothesized that stiffness of the fin rays is important during substrate-contact behaviors. For example, the ventral fin rays that are involved in routine substrate contact in blennies are stiffened by the presence of a lepidotrichial cord (LC) (Brandstätter et al., 1990). This LC is made up of collagenous fibers that are associated with the outer edge of the outer hemitrich of each ventral fin ray. The LC may increase the stiffness of individual fin rays used during behaviors that contribute to body support on the substrate (Brandstätter et al., 1990).

Longhorn sculpin (*Myoxocephalus octodecimspinosus*) are benthic sit-and-wait ambush predators, which avoid predation themselves by remaining stationary for a large proportion of their total time budget (Bidelow and Shroeder, 1953; N.K.T., personal observation). They lack swimbladders and are negatively buoyant in the water (Bidelow and Shroeder, 1953; Taft et al., 2008). They use their large, fan-like pectoral fins to support their weight and rapidly push off from the substrate as well as for swimming in the open water (Taft et al., 2008). It has been shown that the pectoral fin of this species is functionally regionalized, with the more ventral rays being used for direct substrate contact and the dorsal rays being used during slow swimming (Taft et al., 2008). The individual lepidotrichia are also divided into distinct morphological regions (Fig. 1). Specifically, the hemitrichia are unjointed and cylindrical in cross-section proximally. Although most fishes have a short unjointed region at the proximal base of each hemitrichia for muscle attachment, this region is unusually elongate, at least three to five times longer, in longhorn sculpin when compared with extant actinopterygians in which this feature has been studied (Goodrich, 1904; Gosline, 1994). Distal to this unjointed region, the hemitrichia are jointed and crescent-shaped as in pelagic fishes. Unlike the condition in many pelagic fishes, the pectoral fin rays in longhorn sculpin remain unbranched for their entire length. Among longhorn sculpin fin rays, the proportion of the total length of the rays that is unjointed and cylindrical proximally *versus* jointed and crescent-shaped distally varies depending on the location of the ray within the fin (Taft, 2011). Specifically, the ventral rays are shorter and have relatively longer unjointed proximal regions. It is likely that these features of sculpin pectoral fin rays confer a combination of stiffness and flexibility that provide functional advantages necessary for routine substrate contact.

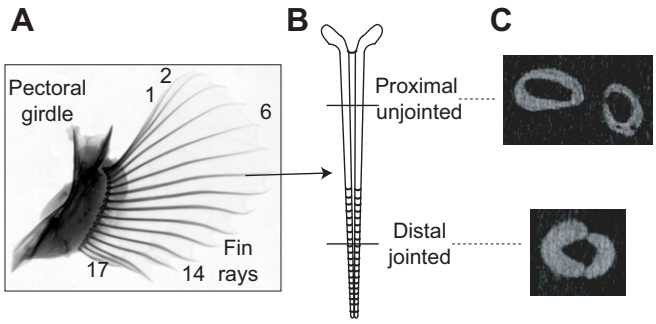

Fig. 1. Illustration of pectoral fin and fin ray morphology. (A) X-ray of the pectoral fin of the longhorn sculpin, *Myoxocephalus octodecimspinosus*, rostral to left. Selected fin rays are numbered, with 1 being the most dorsal and 17 being the most ventral. (B) Simplified diagram of paired hemitrichia making up a single fin ray, proximal at top, lines showing locations of cross-sectional morphology to the right. (C) Images of raw CT slices from a single fin ray of the longhorn sculpin showing the cross-sectional shape of the hemitrichia in the proximal (top) *versus* distal (bottom) regions of the ray.

The broad question we are interested in is: how do the morphological specializations within and among the pectoral fin rays of the longhorn sculpin affect their function? In this study, we will experimentally bend individual lepidotrichia and measure the mean curvature and location of maximum curvature within individual rays and compare these variables among rays within the pectoral fin. Within fin rays, we hypothesize that morphological heterogeneity along the length of individual pectoral fin rays will generate a combination of stiffness proximally and flexibility distally. The absence of joints and the presence of a cylindrical cross-sectional shape always occur together in this species, and we hypothesize that both features will contribute to greater resistance to bending in the proximal region compared with the distal region. The resistance to bending, or flexural stiffness, of a structure is a product of its material properties (Young's modulus) as well as its shape. The effect of a structure's shape on its resistance to bending is quantified by its second moment of area (Vogel, 2003). In this study, we focus on the geometry and shape of the rays as the most important determinants of curvature. Previous research on the stiffness of sculpin ribs suggests that it is the geometry, rather than the material properties, of the bone that is the primary determinant of flexural stiffness (Horton and Summers, 2009). Although we expect the material properties of the collagenous material that unites both the sister hemitrichia and adjacent segments within hemitrichia to affect the curvature of the rays, our focus here is the geometry of the bone.

Within fin rays, we hypothesize that morphological heterogeneity along the length of individual pectoral fin rays will generate a combination of stiffness proximally and flexibility distally. The absence of joints and the presence of a cylindrical cross-sectional shape always occur together in this species, and we hypothesize that both features will contribute to greater resistance to bending in the proximal region compared with the distal region. The size-corrected second moment of area varies along the length of the pectoral fin rays (Taft, 2011). The cylindrical shape of the hemitrichia proximally distributes more of the material away from the neutral plane between sister hemitrichia, which should increase the resistance to bending. In contrast, we predict that the jointed, unbranched distal region of the fin rays will be more flexible as a result of the presence of jointed segments (Etnier, 2001) and

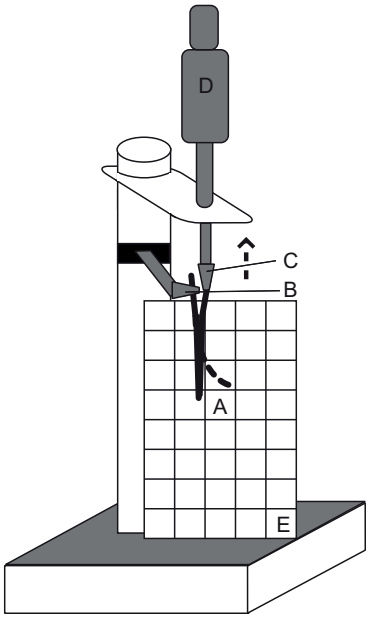

Fig. 2. Experimental apparatus. (A) Fin ray before (solid line) and after (dashed line) relative displacement of hemitrichia; (B) clamp for fixed hemitrich; (C) clamp for 'free' hemitrich; (D) micrometer screw used to displace hemitrichia relative to one another; (E) 5×5 mm grid behind ray for photos.

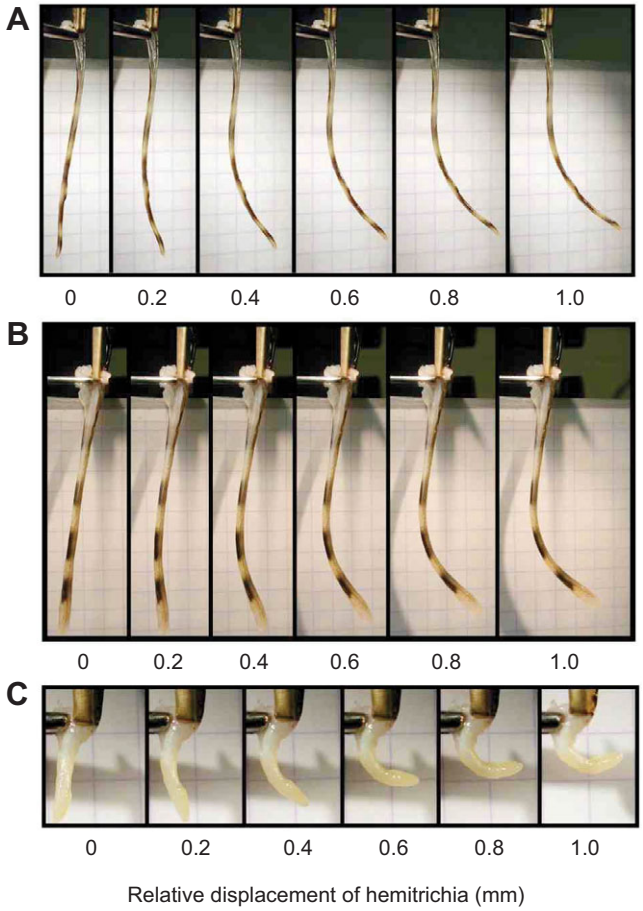

Fig. 3. Photos of bending experiments in three sample fin rays from longhorn sculpin. (A) Dorsal fin ray 2, (B) middle fin ray 8 and (C) ventral fin ray 18. Relative displacement of hemitrichia is shown from left to right starting with a neutral starting position of no displacement to a maximum displacement of 1.0 mm in 0.2 mm intervals. The grid behind fin rays is 5.0×5.0 mm for all photos.

crescent-shaped segments with a lower second moment of area. Among fin rays, we hypothesize that the relative stiffness and flexibility should be correlated with the relative lengths of the proximal and distal regions. Fin rays with longer proximal unjointed regions should resist bending for a greater proportion of their total length and the location of maximum curvature should be more distal.

MATERIALS AND METHODS

Specimens

We collected data on the bending properties of the pectoral fin rays from five individual longhorn sculpins, *Myoxocephalus octodecimspinosus* (Mitchill 1814). Fish were maintained in the laboratory in 1.5 m diameter holding tanks in saltwater (30 ppt) under natural day:night light cycles with a mean water temperature of 10°C (±2°C). The five individuals in this study ranged in total length from 29.00 to 32.75 cm with a mean total length of 30.90 cm. Individuals were euthanized with a lethal dose of MS-222. The pectoral fins were removed from these individuals immediately and placed in Ringer's solution. We dissected each fin ray out of the pectoral fin as needed for each bending trial over the course of no more than 4 h. All animal care and euthanasia were carried out according to IACUC guidelines of the University of Massachusetts, Amherst.

Fin ray bending trials

Our experimental setup was designed to bend individual fin rays by mimicking differential muscle activity on the two sister hemitrichia making up each lepidotrich (Fig. 2). Our experimental design removes the effect of variation in the force and timing of muscle activity acting on individual fin rays. Specifically, regardless of how much force is exerted on the hemitrichia, curvature along the length of each ray is exclusively the result of the relative amount of displacement. In each bending trial, one hemitrich was mounted in a fixed position using a horizontal clamp mounted to a stationary base. We placed this clamp just below the proximal head of the stationary hemitrich where the muscles would attach. Each fin ray was mounted with the distal tip of the ray pointed toward the base of the setup (Fig. 2). The remaining 'free' hemitrich was clamped to a vertically mounted micrometer screw. The height of the micrometer screw was adjusted so that the relative positions of the hemitrichia resulted in a neutral starting position along the length of the ray (Fig. 3). We displaced the free hemitrich relative to the fixed hemitrich at 0.1 mm intervals. The fin rays were mounted in front of a 5×5 mm grid placed no further than 1 cm behind the ray (Figs 2, 3). The fin rays were photographed after each displacement interval using a Nikon Coolpix 990 digital camera. We adjusted the grid and camera after mounting each fin ray before beginning each trial to ensure that bending occurred in the same plane as the grid.

The fin rays were displaced at 0.1 mm intervals until: (1) the fin ray did not bend further with increased displacement or (2) the fin ray began bending out of the plane of the grid and camera. In the course of this experiment we observed that the latter usually occurred at or very close to the point of maximal bending of the fin ray. We performed two bending trials on each fin ray, once with the lateral and once with the medial hemitrich mounted in the stationary position. We randomly alternated which hemitrich was

clamped in the stationary position first both between trials and among individuals. We began bending trials on the most ventral fin ray and conducted tests on every other fin ray plus the most dorsal fin ray. Four of the five individuals had 18 fin rays; the fifth had 17 rays. In all, 10 fin rays from each pectoral fin from five individuals were tested (1, 2, 4, 6, 8, 10, 12, 14, 16 and 17 or 18). Sample photographs from selected fin rays during bending trials can be seen in Fig. 3. We used the image digitizing software Didge (Cullum, 2001) to obtain two-dimensional landmark coordinates for 10 equally spaced points along each fin ray. We set the origin for the coordinates at the first point digitized just below the clamp on the stationary ray (Fig. 3).

Estimation of fin ray curvature

We converted landmark descriptions of rays into estimates of variation in curvature along the length of the rays. In MATLAB (MathWorks, Natick, MA, USA), cubic splines were used to approximate the shape of each ray from our two-dimensional digitized coordinates. Then we calculated the instantaneous curvature of the spline at 101 equidistant points interpolated along the digitized portion of the ray. We calculated curvature along the spline for each ray using the following equation:

$$\kappa = | d\mathbf{T}/ds |, \quad (1)$$

where $\mathbf{T}$ is the unit tangent vector, and s is the arc length of the curve. Curvature (κ) is defined as the change in the unit tangent vector divided by the change in the arc length curve (Taft et al., 2008). One caveat regarding the use of splines to estimate curvature is that they can yield spurious local peaks in curvature at the knots where one piecewise polynomial function is replaced by the next. Taking this into account, we quantified whole-ray curvature in two ways: mean curvature and location of maximum curvature. We estimated the location of maximum curvature as the mean of the location of curvature, weighted by instantaneous curvature. This measure, rather than the location of maximum instantaneous curvature, was chosen in order to smooth out local maxima at spline knots, particularly the knots at the proximal and distal ends of the splines. We described the positions of these points in two ways – as distances, in millimeters, from the proximal base of the ray, and as proportions of the distance between the base and the tip of the ray. In both cases, these distances were measured from the proximal ends of hemitrichia, and not from the location of the most proximal digitized landmark.

Statistical analysis

We examined the effect of the relative displacement on curvature both within and among fin rays. The R statistical environment was used for all analyses in this phase (R Development Core Team, 2011). First, we tested whether rays differed in the amount of relative displacement that was required for the rays to reach maximum curvature. The test used a linear model in which displacement was the response variable, fin ray and stationary hemitrich were fixed categorical effects, and $\log_{10}$ ray length was a covariate. Next, we tested the effect of relative displacement on curvature. We did not know *a priori* how many millimeters it would take to maximally bend each fin ray. Therefore, for our analyses we grouped the displacement trials of each ray into four groups to control for potential variation in the number of millimeters of displacement it took to maximally bend each ray. The continuous ranges of experimental displacements were scaled according to the maximum displacement to which each fin ray/hemitrich combination was subjected. These levels were zero displacement (the resting curvature present in an unloaded ray), zero to one-third of maximum displacement, one-third to two-thirds of maximum displacement and two-thirds to maximum displacement.

We tested whether variation in fin ray length affected how they responded to displacement. To this end, we used a mixed linear model analogous to an ANCOVA in which $\log_{10}$ mean curvature was the response variable, fin ray was the random effect and the fixed-effects model included $\log_{10}$ ray length, displacement group and their interaction. In addition, we used separate repeated-measures ANOVAs to test for differences among rays and hemitrichia in how displacement affected either mean curvature or the locations of greatest curvature. Displacement group was the repeated measure, and the other effects in the models included $\log_{10}$ ray length, and the categorical fixed effects ray, stationary hemitrich and the interaction between ray and hemitrich. We calculated Pillai's trace scores for these models using the 'Anova' function in the R package 'car' (Fox and Weisberg, 2011).

We tested for correlations between two different morphological properties of the rays and displacement-induced changes in ray curvature. Specifically, we were interested in how ray curvature was affected by the relative length of the proximal, unjointed region, as well as the second moment of area at different locations along the fin ray. Our morphological measurements were taken from X-ray computed tomography (CT) scans described in a previous study (Taft, 2011). Because of the time-sensitive and semi-destructive nature of the curvature experiments, it was not possible to perform CT scans of the same fin rays that were used in the bending experiments described here. Although the morphological measurements are taken from different individuals, the relative proportion of the unjointed proximal region was consistent among individuals in a previous study (Taft, 2011). All animals from both studies were adults sampled from the same locality, and we do not expect the pattern of the relative proportions of the unjointed and jointed regions of the ray to vary significantly among individuals in the population.

We hypothesized that location of maximum curvature is correlated with the relative length of the proximal, unjointed region. The unit of replication for this test is the fin ray, so we pooled individuals to calculate the mean length of the unsegmented region and the mean location of greatest curvature for each of the 10 *M. octodecimspinosus* fin rays measured in this analysis. The statistical model for this test was a mixed linear model in which fin ray was a random effect.

We also hypothesized that curvature at four locations along the proximodistal length of each ray is correlated with the predicted size-corrected second moment of area of the hemitrichia at each location predicted from previous research (Taft, 2011). This approach requires estimates of both second moment of area and change in curvature that take into account the fact that area affects the second moment of area and therefore the stiffness of the fin ray. We compared second moment of area with change in curvature at four locations along the length of each ray, located at 10, 30, 50 and 70% of the ray's total length. Morphological measurements were performed as in Taft (Taft, 2011). Mean curvature values were calculated for 10% of the ray's length centered at each location. For example, for the 10% location, we calculated the mean curvature of the region between 5 and 15% of the total length of the ray. Rays differ in cross-sectional area as well as in the way in which shape changes along their length, but here we removed the effect of area to investigate the effect of change in shape on the resistance to bending within a narrow location along the ray. We did this by first calculating an ANCOVA between $\log_{10}$ second moment of area and

$\log_{10}$ area nested within location. Positive residuals from this ANCOVA indicate a greater resistance to bending than would be expected from area alone, with the inverse true for negative residuals. To test our hypothesis that second moment of area affects curvature at each of these locations, we used the mean difference in residual curvature between maximum displacement and no displacement as the response variable in a linear mixed model in which fin ray was the random effect, and location and residual second moment of area, nested within location, were the fixed effects.

RESULTS

On average, sister hemitrichia were displaced 1.06 mm from one another before the end-point criteria were reached. This maximum displacement ranged from 0.4 to 2.5 mm, but deviations from 1 mm were rare. Ray length did not significantly effect maximum displacement (slope=0.16±0.90, $F_{1,74}$=0.20, P=0.65), nor were there significant differences in maximum displacement among rays or hemitrichia.

Mean curvature increased significantly with increased displacement ($F_{3,384}$=39.12, P<0.0001), averaging 0.49±0.16 mm^{-1} higher curvature at maximum displacement than at rest (Fig. 4). In addition, length had a significant negative relationship with curvature, such that longer rays had significantly lower mean curvature (slope=–1.34±0.07 mm^{-2}, $F_{1,384}$=1671, P<0.0001). The slopes of the lines relating ray length and mean ray curvature did not differ among displacement levels ($F_{3,384}$=1.88, P=0.13).

Increased relative displacement caused changes in mean curvature in each ray, but the patterns of change differed among rays (Fig. 5). The effect of displacement on mean curvature showed significant differences among fin rays ($F_{27,234}$≈1.9, P=0.005). Mean curvature varied among fin rays, independent from displacement ($Pillai_9$=0.26, $F_{9,78}$≈3.1, P=0.0030). In agreement with the results described above, mean curvature was significantly affected by the level of displacement ($Pillai_1$=0.79, $F_{3,76}$≈97.0, P<0.0001) and fin ray length ($Pillai_1$=0.14, $F_{1,78}$≈12.6, P=0.0007). There was no significant difference in mean curvature when the lateral *versus* the medial hemitrich was held stationary, although there was a weak trend for curvature to be higher when the medial hemitrich was held stationary ($Pillai_1$=0.035, $F_{1,78}$≈2.8, P=0.096).

The effect of displacement on the location of maximum curvature contrasted with its effect on mean ray curvature. Rays differed significantly from one another in the location of maximum curvature along the proximo-distal length of the ray ($Pillai_9$=0.36, $F_{9,78}$≈4.9, P<0.0001). Within a fin ray, the location of maximum curvature did not vary significantly with increased displacement ($Pillai_1$=0.05, $F_{3,76}$≈1.3, P=0.28). There are no significant differences in location of maximum curvature between hemitrichia.

The mean proportion of ray length that was composed of unsegmented hemitrichia explained 77% of the variation in mean location of maximum curvature on each fin ray (Fig. 6). Maximum curvature was always located distal to the distal tip of the unjointed proximal region (intercept=0.52±0.02, t_8=23.45, P<0.0001). The distance between the end of the unjointed region and the location of maximum curvature was closer among rays with proportionally longer unjointed regions (slope=0.39±0.07, t_8=5.69, P=0.0005).

Each location had its own significant linear relationship between log second moment of area and log cross-sectional area of the hemitrichia at that location (location: $F_{3,32}$=168.2, P<0.0001; location × area: $F_{4,321}$=132.1, P<0.0001; Fig. 7A). After removing the effects of size by using residuals from the ANCOVAs described above, there were significant differences among locations in the relationship between the size-corrected second moment of area of a ray and the amount of change in curvature between zero and maximum displacement (Fig. 7B). First, there were significant differences among locations in their mean change in curvature ($F_{4,31}$=36.1, P<0.0001). The mean change in curvature did not differ from zero at the 10% (–0.02±0.05, t_{31}=–0.36, P=0.73) or 30% locations (0.02±0.04, t_{31}=0.43, P=0.67), whereas the mean curvature change at the 50% (0.22±0.04, t_{31}=5.10, P<0.0001) and 70% locations (0.47±0.04, t_{31}=10.87, P<0.0001) did differ from zero. There was a significant interaction between location and residual second moment of area ($F_{4,31}$=3.08, P=0.030), manifesting in a significant negative relationship (–1.84±0.54, t_{31}=–3.36, P=0.002) between size-corrected second moment of area and size-corrected curvature at the 50% location, which was the only location with a significant relationship of this kind.

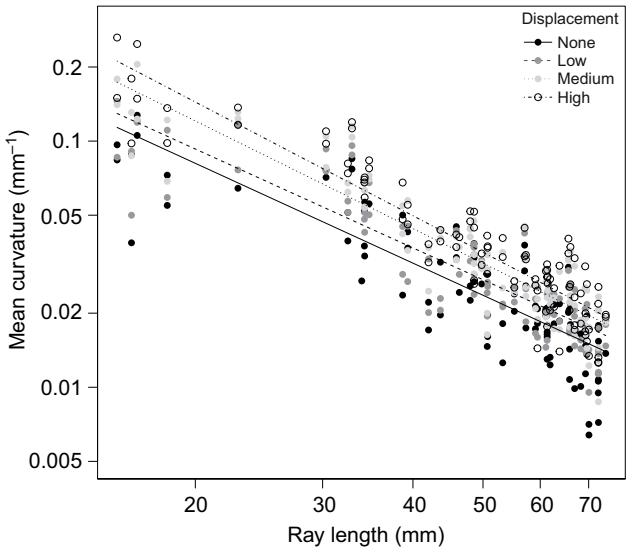

Fig. 4. Mean fin ray curvature and fin ray length. Average curvature of a fin ray is a linear function of its length on a log–log plot. Points represent mean curvature of the fin rays among individuals for a single ray at a single level of displacement. Colors represent curvature at different levels of displacement: none (solid black circles), low (dark gray), medium (light gray) and high (unfilled circles). At different levels of displacement, the lines fit to the length–curvature relationship are parallel, with higher intercepts at greater levels of displacement. Lines shown represent no displacement (solid), low (dashed), medium (dots) and high (dash-dots). Change in curvature due to displacement is independent of ray length.

DISCUSSION

Despite their critical significance in defining fin function, studies of the morphological and functional variation of the fin rays among ray-finned fishes are few, and are largely focused on pelagic fishes. Here, we address this gap by investigating the relationship between morphology and fin ray stiffness in the pectoral fin rays of the benthic longhorn sculpin. We hypothesized that the morphological heterogeneity within and among fin rays would be associated with variation in the relative stiffness and flexibility of the rays individually and as a group. Our results suggest that the presence of an elongate, unjointed proximal region in this species affects both the location and magnitude of curvature and does so both within and among rays. Consequently, variation in stiffness and flexibility among rays within the fin is correlated with variation in the relative lengths of their unjointed regions.

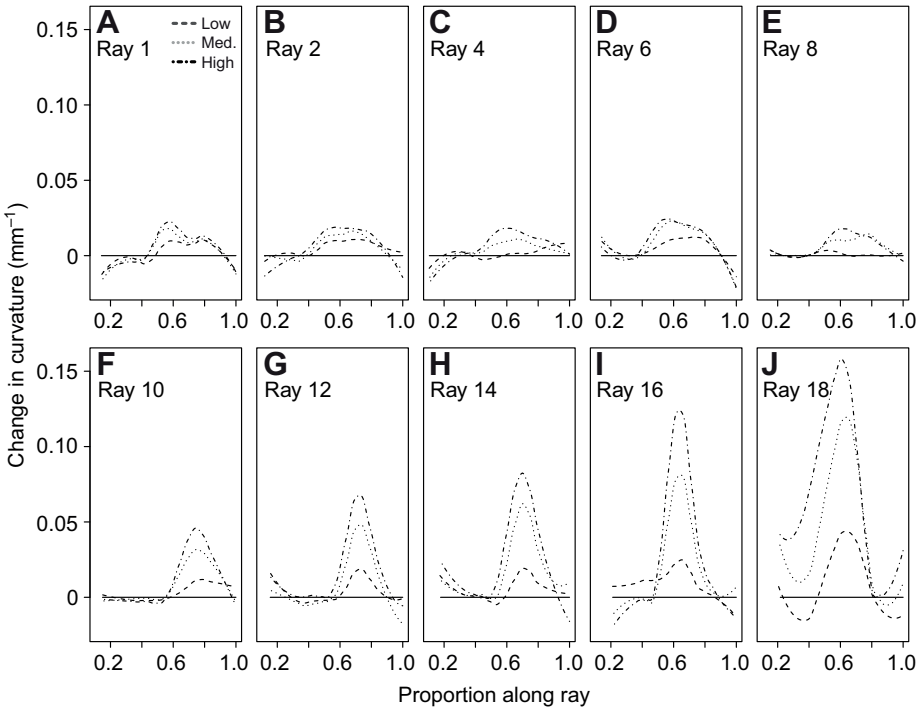

Fig. 5. Locally weighted smooths of instantaneous curvature along each fin ray, showing changes in mean curvature among all fish at four different displacement categories, measured with respect to curvature at rest. Line patterns correspond to the same levels of displacement as in Fig. 4, so that 'no displacement' is a zero line. The location of maximum change in curvature for each ray remains constant across displacement treatments. The magnitude of the change increases with greater amounts of displacement. There is little change in curvature, at any level of displacement, in the proximal region of the rays. Dorsal rays (A–E), which are never involved in substrate contact, show less change in curvature than ventral rays (F–J), which also have more sharply defined peaks in curvature change.

The presence of an elongate unjointed proximal region has several functional consequences. First, the location of maximum curvature is more distal in all but the most dorsal pectoral fin rays of the sculpin when compared with published data from pelagic species (Geerlink and Videler, 1987; Standen and Lauder, 2005) This means that the proximal portions of individual fin rays are stiff, which may provide support that is necessary for bearing the weight of the fish on the bottom. Second, the location of maximum curvature does not change significantly in response to increased displacement in this species, unlike the condition in Nile tilapia (Geerlink and Videler, 1987) and the bluegill sunfish (Lauder et al., 2011) where the location of maximum curvature changes with increased displacement. This proximal stability may also be important for supporting the weight of the fish on the bottom during propping or resting behaviors.

A third consequence of an elongation of the proximal unjointed region in the pectoral rays is the presence of an 'elbow', or region of abrupt increase in curvature. This elbow is only present in the ventral fin rays that, for the most part, have the most elongate proximal unjointed region (Figs 5, 6). This region begins at approximately 50% of the total length in these fin rays, though the location of maximum curvature is more distal (Fig. 5). This elbow may be functionally important during behaviors that help the fish resist displacement from the substrate. For example, the congener of the longhorn sculpin, the father lasher, has been shown to use its ventral fin rays in a finger-like manner to curl around and grip a metal grid to help resist displacement from the substrate in flow (Webb, 1989). This gripping behavior involves pronounced curvature of individual fin rays and would not be possible without the presence of this sharp elbow. Interestingly, our data show that it is at this location that the shape of the ray in cross-section has the most influence on local curvature (Fig. 7B).

The second moment of area, which is related to the shape of the fin rays in cross-section, is correlated with the curvature of the fin rays, but its effect is more local. A previous study of the stiffness of the ribs of a congener of the longhorn sculpin, the great sculpin (*Myoxocephalus polyacanthocephalus*), concluded that it is the geometric arrangement (shape) of the ribs that is the primary determinant of stiffness (Horton and Summers, 2009). Because the shape of the pectoral fin rays of the longhorn sculpin varies significantly along the length of the rays, we explored the effect of the shape, measured by calculating the second moment of area, on curvature at four locations along the length of the rays. As we predicted, there is no significant change in curvature proximally, at distances of 10 or 30% along the ray, where the fin rays are unjointed and cylindrical in cross-section. It is not possible to separate the stiffness due to the absence of joints from the effect of the cylindrical shape in cross-section, but we hypothesize that both morphological features contribute to the stiffness of the hemitrichia. At 70% along the ray, curvature does increase with displacement, but the shape of the hemitrichia is not correlated with this change. It is likely that this is because all of the segments at this location have a similar crescent shape in cross-section. The only location at which there was a significant correlation between second moment of area and curvature was at 50% along the length of the rays. At this location we found that fin rays with a higher second moment of area exhibited a smaller increase in curvature with displacement, whereas those with a lower second moment of area exhibited a more pronounced increase in curvature. The 50% location along the fin ray is functionally significant because it is the point along the length of the rays at which the most abrupt change in curvature begins, particularly among the ventral rays. Our data suggest that variation in shape, here approximated by the size-corrected second moment of area, affects the curvature of the fin rays.

We also found a negative relationship between fin ray length and curvature, such that shorter fin rays exhibited higher curvature (Fig. 4). These rays also possess the proportionally largest unjointed proximal regions, and therefore have the most pronounced 'elbows'. However, we hypothesize that the properties of the collagenous fibers may also limit the total amount of possible shift between the hemitrichia. Recent analysis of the Young's modulus at different locations along the pectoral fin rays of the bluegill sunfish suggests that the elasticity of the pectoral fin rays is within the range of human tendons and that the stiffness of the rays is likely largely determined by the properties of this

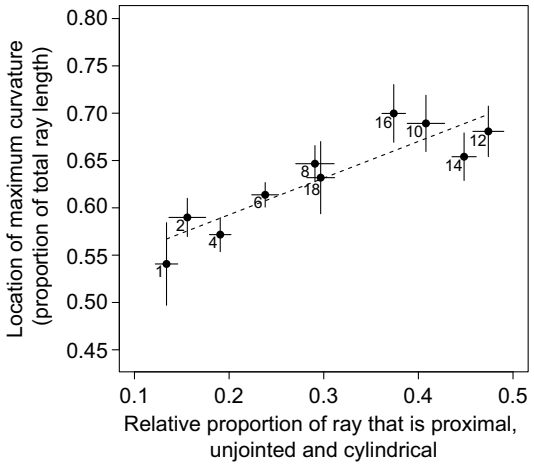

Fig. 6. Relationship of the relative length of the proximal, unsegmented region and the location of maximum curvature among pectoral fin rays. Points represent means of fin rays among all individuals measured. Solid line segments are standard errors, and the dashed line is the fit from a mixed model in which fin ray was the random effect. The proportion unsegmented was measured from CT scans of whole fins from three individuals (see Taft, 2011). The location of greatest curvature was measured from the maximum displacement of each ray for the four individuals in this study.

collagenous material (Lauder et al., 2011). The sister hemitrichia are joined together by short collagenous fibers that run perpendicular to the long axis of the ray. In the pectoral rays of longhorn sculpin, the mean relative shift required to reach maximum displacement was approximately 1 mm. We hypothesize that this distance reflects the stretching limit of the collagenous fibers linking adjacent hemitrichia. The maximum displacement of 1 mm is spread over a larger area in the longer fin rays, leading to a lower curvature of these rays when compared with the shorter fin rays. Our results support earlier work that suggested that the collagenous material connecting the joints making up each hemitrich, as well as those connecting sister hemitrichia, act like tendons by limiting both the relative shift between hemitrichia and the amount of curvature along the length of the ray (Geerlink and Videler, 1987). To date, there have been no formal studies of the mechanical properties of this material. Our data provide additional support for the hypothesis that the material connecting the hemitrichia is a major determinant of fin ray function.

One feature of fin ray morphology that we did not investigate in detail here is the relative number and size of the segments in the distal segmented region of the fin rays. Our unpublished observations on fin rays in the longhorn sculpin, basal actinopterygians (including representatives from *Acipenser*, *Amia*, *Lepisosteus* and *Polypterus*) and a large sample of scorpaeniform fishes suggests that this is a highly variable feature that we hypothesize should have significant functional consequences. For example, our preliminary data suggests that in the longhorn sculpin, the segments of the ventral rays are shorter relative to the overall length of the fin ray than those in more dorsal rays, which may be a factor contributing to their higher curvature and flexibility. Previous work examining the material properties in segmented crinoid arms and crustacean antennae suggests that the diameter of a segmented structure has the greatest effect on its stiffness (Etnier, 2001). Increases in joint density (number of joints between segments per millimeter of beam length) did decrease stiffness of crinoid arms, but not crustacean antennae. These structures do not have the more complex paired arrangement of the hemitrichia that make up individual fin rays, but suggest that the relative size and number of segments can affect the material properties of segmented biological beams (Etnier, 2001). Future work that includes data on the functional consequences of variation in segment size and number will be important for understanding overall flexibility and curvature of vertebrate lepidotrichia.

We have demonstrated that morphological variation is correlated with variation in the relative stiffness and flexibility in and among the pectoral fin rays of the longhorn sculpin. The most ventral fin

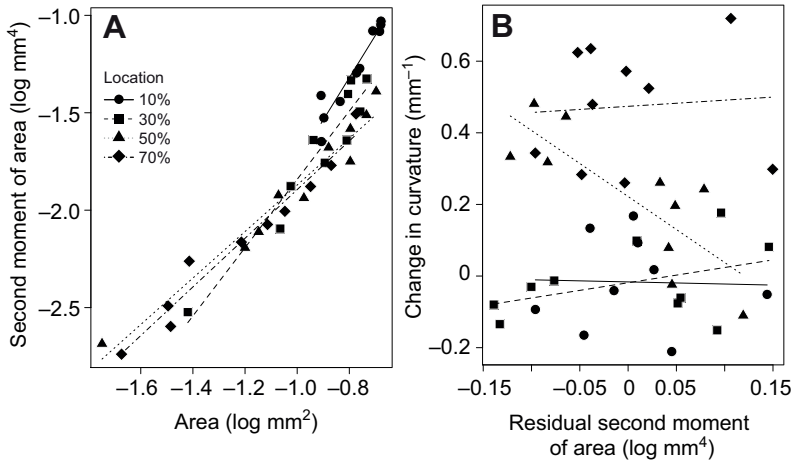

Fig. 7. The effect of local shape on local change of curvature in longhorn sculpin pectoral fin rays. Change in curvature, area and second moment of area were measured on 10 fin rays at four locations along the proximodistal length of the rays. Change in curvature is the difference in mean curvature at maximum displacement and no displacement, measured in the 10% interval around the center of the location. Each location (10%, circles, solid lines; 30%, squares, dashed lines; 50%, triangles, dotted lines; 70%, diamonds, dot-dash lines) of the ray's length had a separate significant linear relationship between log area and log second moment of area (A). The relationship between change in curvature and residual second moment of area differs among the four locations (B). There is no significant change in curvature at all at either of the two most proximal locations, 10 and 30%. Change in curvature is significantly greater than zero at the most distal location, 70%, but is not significantly affected by shape at that location. In contrast, local shape significantly affects local curvature at 50%, where rays with greater size-corrected second moments of area at that location have a lower change in curvature.

rays, which are used for routine substrate contact, have both a larger stiff proximal region and a more highly curved and potentially more flexible distal tip. Both of these features are correlated with the same morphological feature, a proximal region in which the hemitrichia are unjointed and cylindrical in cross-section. Previous studies of benthic fish fin morphology have hypothesized that separate regions of stiffness and flexibility are adaptive for support and substrate contact when the fish is on the bottom. We hypothesize that the morphological specialization of the pectoral fin rays of the longhorn sculpin is associated with routine substrate contact because these patterns are much more pronounced in the ventral fin rays that are used for this purpose. The more dorsal fin rays that are not used for substrate contact more closely resemble those of pelagic fishes both functionally and morphologically. Accordingly, the dorsal rays lack the pronounced elbow and have a more proximal location of maximum curvature, like fin rays of pelagic fishes. To date, this feature has only been described for this species among the extant ray-finned fishes. However, we predict that, given its functional significance, the presence of a stiff proximal region may be relatively common among benthic fishes. Future work on a phylogenetically and behaviorally diverse sample of fishes will provide new insight into how fin ray morphology affects whole-fin function.

ACKNOWLEDGEMENTS

We would like to thank John Clark of City Gear (Irvington, NY, USA) for his invaluable assistance in constructing our bending apparatus. We thank Normandeau Associates for specimens of longhorn sculpin. We would also like to thank George Lauder, Gary Gillis, Stephen McCormick, Cristina Cox Fernandes, Heather King and Kerin Claeson for helpful comments about the manuscript, and Kapi Monoyios for helpful comments on Fig. 1. We also thank two anonymous reviewers for their useful comments, which improved this manuscript.

FUNDING

This study was funded in part through a scholarship to N.K.T. from the Jane H. Bemis Scholarship Fund through the Massachusetts Natural History Collections at the University of Massachusetts Amherst.

REFERENCES

Alben, S., Madden, P. G. and Lauder, G. V. (2007). The mechanics of active fin-shape control in ray-finned fishes. *J. R. Soc. Interface* **4**, 243-256.

Bidelow, H. B. and Shroeder, W. C. (1953). Longhorn sculpin *Myoxocephalus octodecimspinosus* (Mitchill) 1815. In *Fishes of the Gulf of Maine* (ed. B. B. Collette and G. Klein-MacPhee), pp. 47-50. Washington, DC: United States Government Printing Office.

Brandstätter, R., Misof, B., Pazmandi, C. and Wagner, G. P. (1990). Microanatomy of the pectoral fin in blennies (Blenniini, Blennioidea, Teleostei). *J. Fish Biol.* **37**, 729-743.

Cullum, A. (2001). *Didge: Image Digitizing Software*. Omaha, NE: Parthenogenic Products.

Etnier, S. A. (2001). Flexural and torsional stiffness in multi-jointed biological beams. *Biol. Bull.* **200**, 1-8.

Fox, J. and Weisberg, S. (2011). *An R Companion to Applied Regression*, 2nd edn. Thousand Oaks, CA: Sage.

Geerlink, P. J. and Videler, J. J. (1986). The relation between structure and bending properties of teleost fin rays. *Neth. J. Zool.* **37**, 59-80.

Goodrich, E. S. (1904). On the dermal fin-rays of fishes – living and extinct. *Q. J. Microsc. Sci.* **47**, 465-518.

Gosline, W. A. (1973). *Functional Morphology and Classification of Teleostean Fishes*. Honolulu, HI: University Press of Hawaii.

Gosline, W. A. (1994). Function and structure in the paired fins of scorpaeniform fishes. *Environ. Biol. Fishes* **40**, 219-226.

Horton, J. M. and Summers, A. P. (2009). The material properties of acellular bone in a teleost fish. *J. Exp. Biol.* **212**, 1413-1420.

Lauder, G. V. and Madden, P. G. A. (2007). Fish locomotion: kinematics and hydrodynamics of flexible foil-like fins. *Exp. Fluids* **43**, 641-653.

Lauder, G. V., Madden, P. G., Mittal, R., Dong, H. and Bozkurttas, M. (2006). Locomotion with flexible propulsors: I. Experimental analysis of pectoral fin swimming in sunfish. *Bioinspir. Biomim.* **1**, S25-S34.

Lauder, G. V., Madden, P. G. A., Tangorra, J. L., Anderson, E. and Baker, T. V. (2011). Bioinspiration from fish for smart material design and function. *Smart Mater. Struct.* **20** 13.

R Development Core Team (2011). R: a language and environment for statistical computing. Vienna: R Foundation for Statistical Computing. Available at www.r-project.org.

Standen, E. M. and Lauder, G. V. (2005). Dorsal and anal fin function in bluegill sunfish *Lepomis macrochirus*: three-dimensional kinematics during propulsion and maneuvering. *J. Exp. Biol.* **208**, 2753-2763.

Taft, N. K. (2011). Functional implications of variation in pectoral fin ray morphology between fishes with different patterns of pectoral fin use. *J. Morphol.* **272**, 1144-1152.

Taft, N. K., Lauder, G. V. and Madden, P. G. A. (2008). Functional regionalization of the pectoral fin of the benthic longhorn sculpin during station holding and swimming. *J. Zool.* **276**, 159-167.

Vogel, S. (2003). *Comparative Biomechanics: Life's Physical World*. Princeton, NJ: Princeton University Press.

Webb, P. W. (1989). Station-holding by three species of benthic fishes. *J. Exp. Biol.* **145**, 303-320.